

See discussions, stats, and author profiles for this publication at: <https://www.researchgate.net/publication/290348316>

Vacuum and multiphase screw pump rotor profiles and their calculation models

Article · January 2006

CITATIONS

2

READS

549

4 authors:



Nikola Stosic

City, University of London

172 PUBLICATIONS 1,101 CITATIONS

[SEE PROFILE](#)



Ian Kenneth Smith

City, University of London

120 PUBLICATIONS 852 CITATIONS

[SEE PROFILE](#)



Ahmed Kovacevic

City, University of London

155 PUBLICATIONS 803 CITATIONS

[SEE PROFILE](#)



Elvedin Mujic

Bitzer

48 PUBLICATIONS 131 CITATIONS

[SEE PROFILE](#)

Some of the authors of this publication are also working on these related projects:



Grid Generation in positive displacement screw machines [View project](#)



Development of design tools for screw compressors [View project](#)

Vacuum and Multiphase Screw Pump Rotor Profiles and Their Calculation Models

N. Stosic, I. K. Smith, A. Kovacevic and E. Mujic

City University, London, UK

Abstract

A series of rotor profiles for vacuum and multiphase pumps was created to check the suitability of standard screw compressor design software to cope with the specific requirements of these machines. Performances calculations were carried out on them and the results, presented, show good agreement with published experimental data.

Nomenclature

A	Area of passage cross section, oil droplet total surface
a	Speed of sound
C	Rotor centre distance, specific heat capacity
d	Oil droplet Sauter mean diameter
x,y,z	Rotor Cartesian coordinate directions
h	Specific enthalpy $h=h(\theta)$, convective heat transfer coefficient between oil and gas
k	Time constant
m	Mass
\dot{m}	Inlet or exit mass flow rate $\dot{m} = \dot{m}(\theta)$
p	Rotor lead, Fluid pressure in the working chamber $p = p(\theta)$
\dot{Q}	Heat transfer rate between the fluid and the compressor surroundings $\dot{Q} = \dot{Q}(\theta)$
r	Rotor radius
s	Distance between the pole and rotor contact points
T	Torque, Temperature
U	Internal energy
W	Work output
V	Local volume of the compressor working chamber $V=V(\theta)$
\dot{V}	Volume flow

x Rotor coordinate, Dryness fraction

y Rotor coordinate

Greek letters

η_i Adiabatic efficiency

η_t Isothermal efficiency

η_v Volumetric efficiency

θ Male rotor angle of rotation

ζ Compound, local and point resistance coefficient

ω Angular speed of rotation of the male rotor

Prefixes

d Differential

Δ Increment

Subscripts

f Saturated liquid

g Saturated vapour

in Fluid inflow

ind Indicator

l Leakage

oil Oil

out Fluid outflow

p Previous step in iterative calculation

w pitch circle

1 male rotor, upstream condition

2 female rotor, downstream condition

Introduction

Vacuum pumps and multiphase pumps have similar rotor profile shapes. They are usually made with very large wrap angles to allow for a transport, or constant volume phase in the compression process. This is needed in order to split the pressure difference into several portions so that internal leakage is minimized and hence relatively large clearances can be maintained between the rotors and between rotors and machine housings. These are needed, in the case of vacuum pumps, which operate at very low pressures, in order to allow for molecular flow effects. In the case of multiphase pumps, large clearances are needed to permit the free passage of relatively large solid particles, which may be flowing through them. As is shown in this paper, a common approach to their design and use of the same software for their calculation is therefore possible.

To retain high volumetric efficiencies with large clearances, the pressure difference between the lobes must be minimised while the flow capacity is maximised. Consequently, screw rotor profiles for vacuum and multiphase pumps should be designed to achieve the highest displacement and the highest possible ratio between the flow and leakage areas. Since the flow area and the ratio between the flow and leakage areas are both inversely proportional to the number of rotor lobes, a 1-1 configuration, with one lobe each in the main and gate rotors, seems to be the best choice for such machines. For ease of machining and simplicity of manufacture both rotors may have the same profile. These assumptions then lead to a family of shapes which may be considered for these applications. To determine the character of these profiles, the envelope theory of gearing has been used for the computer generation of a range of 1-1 screw rotor shapes.

A standard software package, which models the flow and thermodynamic processes within screw machines, was modified to cover both the vacuum and multiphase pump processes by introducing molecular and particle flow effects within the calculations. Performance estimates were thus obtained and compared for the various rotor profiles generated. The machine designs were then optimised to achieve the best volumetric and adiabatic efficiencies.

Rotor Generation

Screw pump rotors usually have parallel axes and a uniform lead. Their centre distance $C=r_{1w}+r_{2w}$, where r_{1w} and r_{2w} are rotor pitch circle radii. Rotors make line contact and the meshing criterion in the transverse plane perpendicular to their axes is the same as that of spur gears.

The profile point coordinates in the transverse plane of one rotor, x_{01} and y_{01} and their first

derivatives in respect to rotor parameter t , either $\frac{\partial x_{01}}{\partial t}$ and $\frac{\partial y_{01}}{\partial t}$ or $\frac{dy_{01}}{dx_{01}}$ must be known for

the generation of the meshing points, as presented in Fig. 1. These may be specified on either the main or gate rotors or in sequence on both, as well as on the rack. A meshing condition based on the envelope procedure is:

$$\frac{dy_{01}}{dx_{01}} \left(ky_{01} - \frac{C}{i} \sin \theta \right) + kx_{01} + \frac{C}{i} \cos \theta = 0 \quad (1)$$

where i is the gear ratio and $k=1-1/i$. Once obtained numerically from (1), the distribution of θ along the profile may be used to calculate the meshing rotor profile point coordinates, as

well as to determine the sealing lines between the two rotors. The rotor rack coordinates may also be calculated from the same θ distribution.

The meshing profile equations of the opposite rotor in the transverse plane are calculated as:

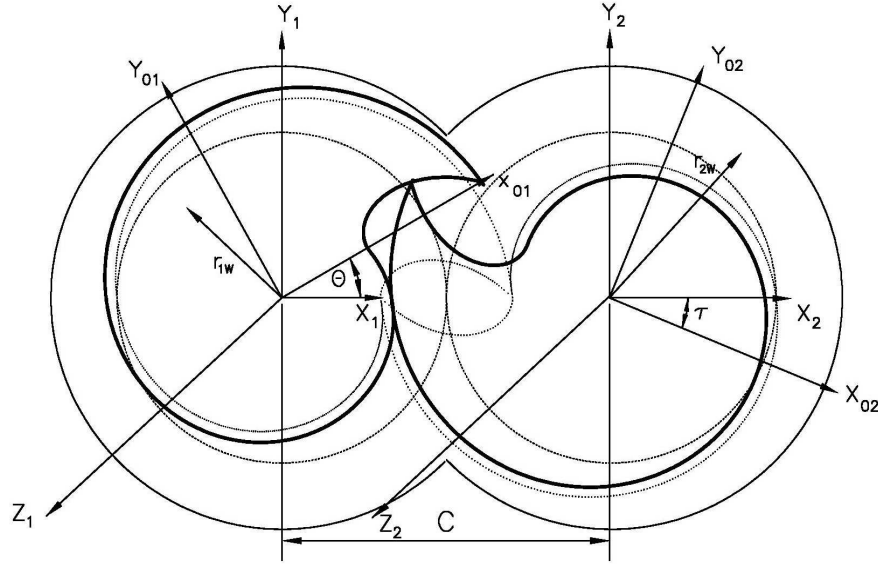


Fig. 1: Screw pump rotors and their coordinate systems

$$\begin{aligned} x_{02} &= x_{01} \cos k\theta - y_{01} \sin k\theta - C \cos \frac{\theta}{i} \\ y_{02} &= x_{01} \sin k\theta + y_{01} \cos k\theta + C \sin \frac{\theta}{i} \end{aligned} \quad (2)$$

The rack coordinates can be obtained uniquely from Eq. (2) if the rack-to-rotor gear ratio i tends to infinity:

$$\begin{aligned} x_{0r} &= x_{01} \cos \theta - y_{01} \sin \theta \\ y_{0r} &= x_{01} \sin \theta + y_{01} \cos \theta - r_{1w} \theta \end{aligned} \quad (3)$$

If the primary curves are given on the rack, their coordinates x_{0r} and y_{0r} , as well as their first derivatives, $\frac{\partial x_{0r}}{\partial t}$ and $\frac{\partial y_{0r}}{\partial t}$, or $\frac{dy_{0r}}{dx_{0r}}$ should be known and the generated curves will be calculated at the rotors as:

$$\begin{aligned} x_{01} &= x_{0r} \cos \theta - (y_{0r} - r_{1w}) \sin \theta \\ y_{01} &= x_{0r} \sin \theta + (y_{0r} - r_{1w}) \cos \theta \end{aligned} \quad (4)$$

after the meshing condition is obtained from:

$$\frac{dy_{0r}}{dx_{0r}}(r_{1w}\theta - y_{0r}) - (r_{1w} - x_{0r}) = 0 \quad (5)$$

The rack meshing condition θ can be solved directly.

A variety of primary arc curves basically offers a general procedure. Only the primary arcs should be given. The secondary arcs are not derived but they are evaluated automatically by means of the numerical procedure.

Since there exists a clearance gap between the rotors, the sealing line consists of the locus of the points of the most proximate rotor position. Its coordinates are x_1 , y_1 and z_1 and they are calculated for the same θ distribution.

One set of vacuum or multiphase pump rotors with an involute profile is presented in Fig. 2. More on the screw compressor rotor profiling can be found in Stosic et al, 2005, [3].

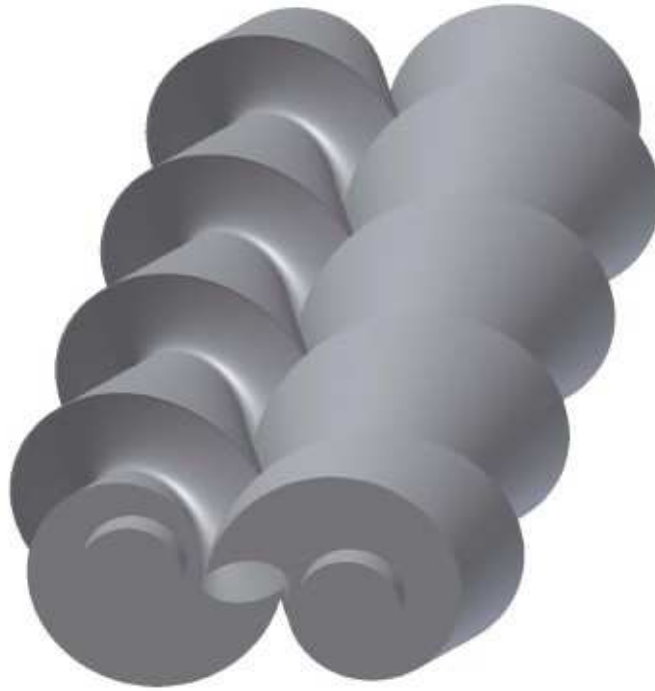


Fig. 2: 3-D sketch of a screw pump rotor with involute profile

Performance Calculation

A standard algorithm for the calculation of screw compressors, represented by a set of differential equations which describe the physics of the complete process in a compressor

was used to estimate the screw pump performance. The equation set consists of the differential equations for energy and mass continuity and a number of algebraic equations, such as those defining instantaneous volume as a function of time, as well as an equation of state for the working fluid. These are applied for each phase of the process that the fluid is subjected to, namely: suction, transport, compression and discharge.

Various simplifications of the equations, that have often been applied in the past in order to achieve a more efficient and economical numerical solution of the equation set, are in this case less significant, and it is possible to use the model to determine whether or not neglecting some of the terms in the equations and other simplifications are justified.

The model accounts for a number of “real-life” effects which may have significant influence on the final estimation of the performance of a real compressor. These provisions ensure the generality of the model and its suitability for a wider range of applications.

The working chamber of a screw machine is a typical example of an open thermodynamic system in which the mass flow varies with time. Internal energy is the derived variable. This practice was found computationally beneficial in evaluating the properties of real fluids, compared with previously more conventional methods, based on the use of enthalpy as the dependent variable. All the remaining thermodynamic and fluid properties within the machine cycle are then derived from it and the computation is carried out through several cycles until the solution converges

The equation of conservation of internal energy $U(\theta)$ can be written as:

$$\omega \left(\frac{dU}{d\theta} \right) = \dot{m}_{in} h_{in} - \dot{m}_{out} h_{out} + \dot{Q} - \omega p \frac{dV}{d\theta} \quad (6)$$

where θ is angle of rotation of the main rotor, $h=h(\theta)$ is the specific enthalpy, $\dot{m} = \dot{m}(\theta)$ is the mass flow rate, $p=p(\theta)$ is the fluid pressure in the working chamber control volume, $\dot{Q} = \dot{Q}(\theta)$, is the heat transfer between the fluid and the compressor surroundings and $\dot{V} = \dot{V}(\theta)$, is the local volume of the compressor working chamber. In the above equation the subscripts “in” and “out” denote the fluid inflow and outflow, respectively. The total fluid enthalpy inflow consists of the following components: $\dot{m}_{in} h_{in} = \dot{m}_{suc} h_{suc} + \dot{m}_{l,g} h_{l,g} + \dot{m}_{liq} h_{liq}$, where subscript “l,g”, “suc” and “liq” denote leakage gain, suction conditions, and liquid carried over, respectively. The total fluid enthalpy outflow can be expressed as: $\dot{m}_{out} h_{out} = \dot{m}_{dis} h_{dis} + \dot{m}_{l,l} h_{l,l}$, where the subscripts “l,l” and dis denote leakage loss and

discharge conditions with \dot{m}_{dis} denoting the discharge mass flow rate of the gas together with the liquid transported.

The right hand side of the energy equation consists of the following terms which are modelled: the heat exchanged between the fluid and the compressor screw rotors and the casing, the energy gain due to the gas inflow into the working volume, which is represented by the product of the mass intake and its averaged enthalpy, the total enthalpy inflow, which is further corrected by the enthalpy brought into the working chamber by the injected oil, the energy loss due to the gas outflow from the working volume, which is defined by the product of the mass outflow and its averaged gas enthalpy and the thermodynamic work supplied to the gas during the compression process, which is expressed by the term $p \frac{dV}{d\theta}$.

In vacuum pumps, the compression work is relatively small compared with the mechanical, indicator and leakage losses and the heat transfer to the surrounding and, indeed its theoretical value tends to zero for very low inlet pressures. Moreover, in reality the transport phase at constant volume is accompanied by leakages, which fill the working chamber, thereby increasing the pressure in it and thus it replicating internal compression.

However, the heat transfer, which depends on the temperature difference, the heat transfer surface area and the heat transfer coefficients, has a finite value regardless the power input. This means that vacuum pumps are well cooled. This has even greater significance at low pressures, where the gas kinematic viscosity has very high values, thus ensuring that the heat transfer coefficients between the gas and the rotors and the housing are high. It follows that the finite value of the heat transfer rate compensates for the small power inputs and the internal losses. Accordingly, the working temperature in a vacuum pump is stabilized at reasonable levels. This feature is well accounted for in the standard version of screw compressor design software.

Sludge flow, which accompanies the gas compressed in multiphase pumps is usually incompressible and may be volatile. Therefore its phase may change during the pumping process. The liquid portion of the sludge will behave as incompressible fluid consuming relatively small power despite its high mass flow, interacting with the gas flow only through internal heat transfer, while the vapour phase will behave as a gas, contributing significantly to the power consumption. Both of these phenomena are fully accounted for in the original mathematical model of the screw compressor process. A description of the passive scalar transport approach, used in this paper, may be found in Kovacevic et al, 2006, [2].

The mass continuity equation for $m(\theta)$ is given as:

$$\omega \frac{dm}{d\theta} = \dot{m}_{in} - \dot{m}_{out} \quad (7)$$

The mass inflow rate can be expressed as $\dot{m}_{in} = \dot{m}_{suc} + \dot{m}_{l,g} + \dot{m}_{liq}$, while that for the outflow rate can be written as $\dot{m}_{out} = \dot{m}_{dis} + \dot{m}_{l,l}$. Each of the mass flows satisfies the continuity equation $\dot{m} = \rho w A$, where w denotes fluid velocity, ρ - fluid density and A - the flow cross-section area. The instantaneous density $\rho = \rho(\theta)$ is obtained from the instantaneous mass m , trapped in the control volume, and the size of the corresponding instantaneous volume V and is expressed as $\rho = m/V$.

The leakages in a screw machine amount to a substantial part of the total flow rate and therefore play an important role because they influence the process both by affecting the compressor mass flow rate or compressor delivery, i.e. volumetric efficiency and the thermodynamics of the compression work efficiency. Computation of the leakage velocity follows from approximate consideration of the fluid flow through the clearances. The process is essentially flow with friction and heat transfer. The mass flow of leaking fluid is expressed by the continuity equation: $\dot{m}_l = \mu_l \rho_l w_l A_g$, where ρ and w are density and velocity of the leaking gas, $A_g = l_g \delta_g$ the clearance gap cross-sectional area, l_g leakage clearance length, sealing line, δ_g leakage clearance width or gap, $\mu = \mu(\text{Re}, \text{Ma})$ the leakage flow discharge coefficient.

Four different sealing lines are distinguished in screw machines: the leading tip sealing line, formed by the main and gate rotor forward tip and casing, the trailing tip sealing line, formed by the rotor reverse tip and casing, the front sealing line, between the discharge rotor front and the housing and the interlobe sealing line, between the rotors.

All the sealing lines have clearance gaps that form leakage areas. Additionally, the tip leakage areas are accompanied by the blow-hole areas.

According to the type and position of the leakage clearances, five different leakages can be identified. Four of these are: the losses through the trailing tip, the sealing, the front sealing and the gains through the leading and front sealing. The fifth, 'through-leakage' does not directly affect the process in the working chamber, but passes through it from the discharge plenum towards the suction port.

The computation of the leaking gas velocity follows from the momentum equation, which accounts for the fluid-wall friction:

$$w_l dw_l + \frac{dp}{\rho} + f \frac{w_l^2}{2} \frac{dx}{D_g} = 0 \quad (8)$$

where $f(\text{Re}, \text{Ma})$ is the friction coefficient, which is dependent on the Reynolds and Mach numbers, D_g is the effective diameter of the clearance gap, $D_g \approx 2\delta_g$, and dx is the length increment. From the continuity equation and assuming that $T \approx \text{const}$ in order to eliminate gas density in terms of pressure, the equation can be integrated in terms of pressure from the high pressure side at position 2 to the low pressure side at position 1 of the gap to yield:

$$\dot{m}_l = \rho_l w_l A_g = A_g \sqrt{\frac{p_2^2 - p_1^2}{a^2 \left(\zeta + 2 \ln \frac{p_2}{p_1} \right)}} \quad (9)$$

where $\zeta = f L_g / D_g + \Sigma \xi$, characterizes the leakage flow resistance, with L_g , the clearance length in the leaking flow direction, f , the friction factor and ξ , the local resistance coefficient. ξ can be evaluated for each clearance gap as a function of its dimensions and its shape and flow characteristics. The speed of sound is a .

The full procedure requires the model to include the friction and drag coefficients in terms of the Reynolds and Mach numbers for each type of clearance.

Likewise, the working fluid friction losses can also be defined terms of the local friction factor and fluid velocity related to the tip speed, density, and elementary friction area. At present the model employs the value of ξ , in terms of a simple function for each particular compressor type, and uses it as an input parameter.

The equations of energy and continuity are solved to obtain $U(\theta)$ and $m(\theta)$. Together with $V(\theta)$, the specific internal energy, $u=U/m$, and the specific volume, $v=V/m$, are now known.

For an ideal gas: $T = (\gamma - 1) \frac{u}{R}$ $p = \frac{RT}{v}$. In this case T and p are calculated explicitly.

Numerical solution of the mathematical model of the physical process in the compressor provides a basis for more exact computation of all desired integral (bulk) characteristics, with a satisfactory degree of accuracy, and, in that respect, is superior than the empirical integral approach. The most important of these properties are the compressor mass flow rate \dot{m} [kg/s], the indicated power P_{ind} [kW], specific indicated power P_s [kJ/kg], volumetric

efficiency η_v , adiabatic efficiency η_a , isothermal efficiency η_t and other efficiencies, and the power utilization coefficient and the indicated efficiency η_i .

All other design software features, such as profile and working parameter optimisation, pressure load calculations and interfaces to CAD systems are retained and are fully functional. More about the models used in this paper can be found in Stosic et al, 2005, [3].

Review of Screw Pump Profiles

A number of profiles for screw pumps have been created to illustrate the ability of the standard screw compressor software to be used in this specific application. The screw pump design imposed the requirement that both rotors must be identical, in order to be manufactured by a single tool. Both rotor and rack generation procedures were used; the first for circular profiles and the latter for involute profiles.

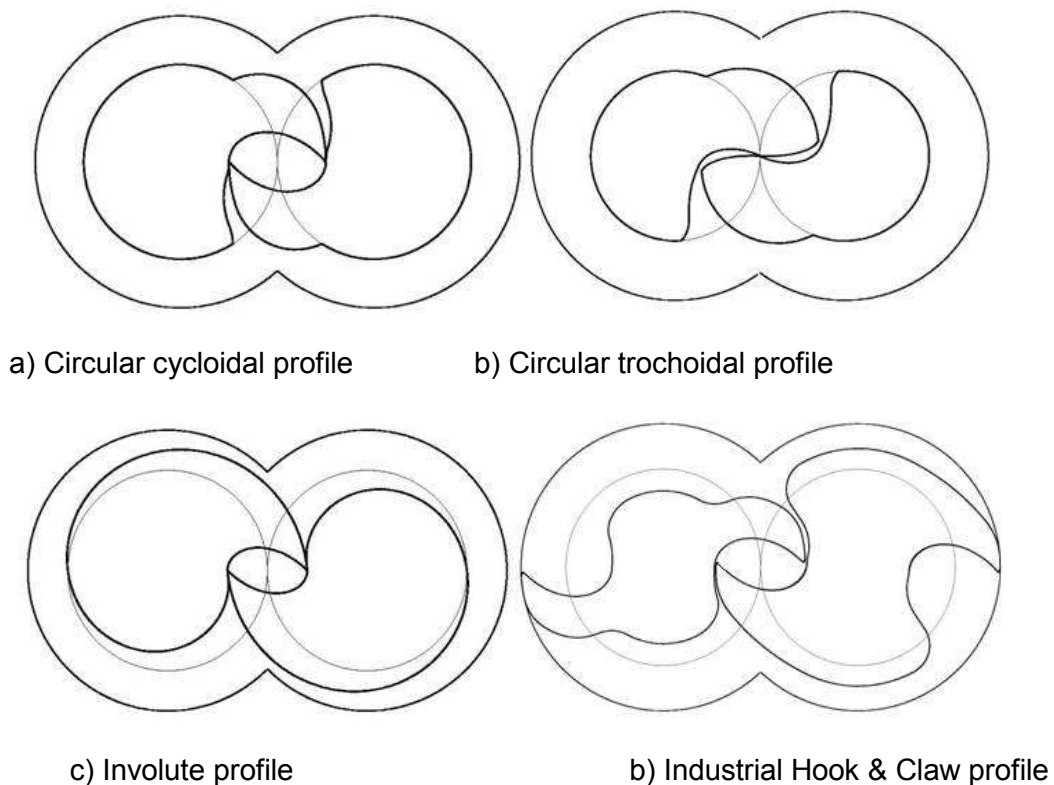


Fig. 3: Typical screw pump rotor profiles

The profiles presented in Fig. 3 are typical shapes which may be used for vacuum and multiphase pump application. The circular profile assures a small blow-hole area.

Unfortunately, it retains a high carryover, as is the case for the involute profile and the industrial hook and claw profiles. The trochoidal profile, b) has a small carry over. However, it has a large blow-hole area.

Multilobe profiles, some of them presented in Fig. 4, are not common in industrial practice. However, they have some distinct advantages, because they increase the number of working chambers for the same wrap angle thus reducing the pressure difference between them.

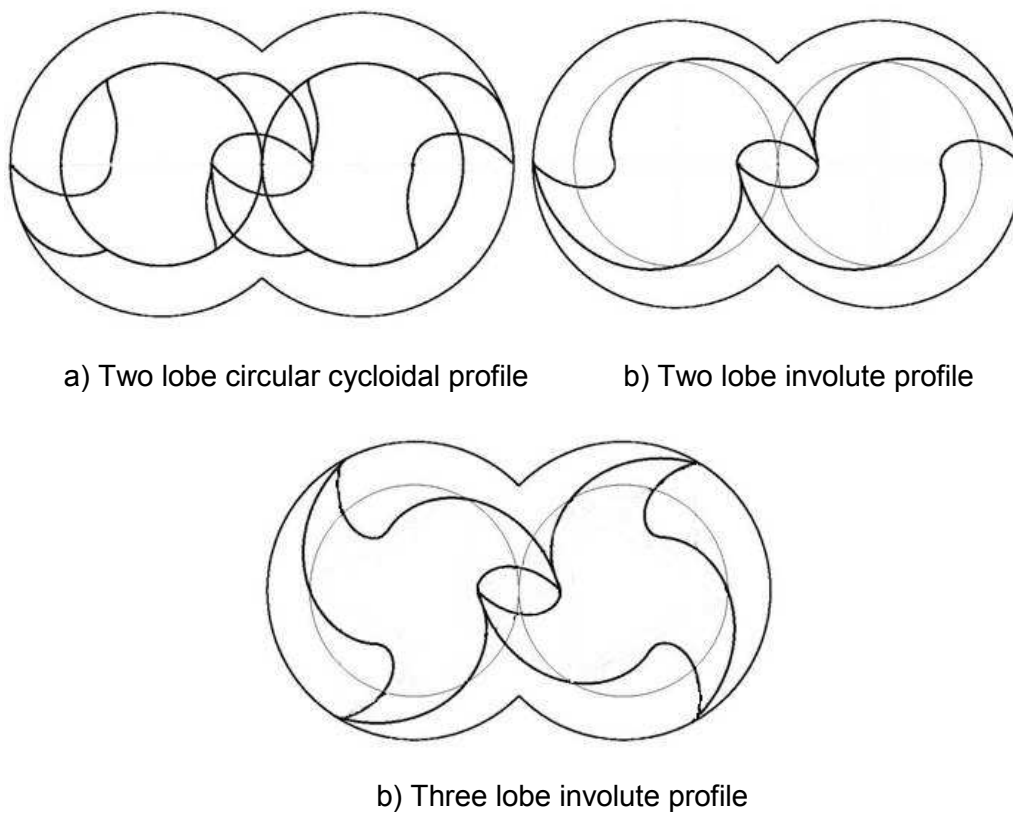


Fig. 4: Multilobe screw pump rotor profiles

Calculation Examples

Calculation results for the multiphase pump are compared with the experimental values obtained by Feng et al, 2001 [1], which are presented in column 5 of Table 1, while those for vacuum pump are presented in Table 1. The calculation results follow the experimental results reasonably well.

Table 1: Performance of multiphase pump

P _{disch}	Rpm	m ³ /min	η_v	$\eta_{v \text{ exp}}$	kW	kW/m ³ /min	η_a
bar							
	1501	2.253	0.72	0.72	12.779	5.673	0.5
4	1801	2.803	0.748	0.74	14.794	5.277	0.537
	2101	3.349	0.766	0.76	16.823	5.023	0.564
	1501	2.167	0.693	0.69	19.585	9.038	0.431
6	1801	2.725	0.727	0.71	22.658	8.314	0.469
	2101	3.277	0.749	0.73	25.742	7.854	0.496
	1501	2.093	0.67	0.67	26.317	12.573	0.376
8	1801	2.659	0.709	0.70	30.454	11.453	0.413
	2101	3.218	0.736	0.71	34.600	10.751	0.44
	1501	2.027	0.648	0.65	33.022	16.295	0.333
10	1801	2.601	0.694	0.66	38.237	14.7	0.369
	2101	3.168	0.724	0.68	43.457	13.716	0.396
	1501	1.966	0.629		39.716	20.206	0.298
12	1801	2.549	0.68		46.020	18.051	0.334
	2101	3.126	0.714		52.326	16.739	0.36
	1501	1.909	0.611	0.63	46.410	24.316	0.27
14	1801	2.502	0.667	0.65	53.801	21.499	0.305
	2101	3.089	0.706	0.66	61.208	19.815	0.331

Table 2: Performance of vacuum pump

P_{suct}	rpm	m^3/min	η_v	kW	$\text{kW}/\text{m}^3/\text{min}$	η_a
bar						
0.01	3001	3.873	0.62	5.013	1.294	0.123
0.03	3001	4.68	0.749	5.021	1.073	0.281
0.05	3001	4.886	0.782	5.016	1.027	0.385
0.07	3001	4.979	0.797	5.001	1.004	0.463
0.09	3001	5.026	0.804	4.97	0.989	0.525
0.11	3001	5.039	0.806	4.916	0.976	0.578
0.13	3001	5.007	0.801	4.825	0.964	0.623
0.15	3001	5.23	0.837	5.237	1.001	0.629
0.17	3001	5.235	0.838	5.134	0.981	0.667
0.19	3001	5.24	0.838	5.094	0.972	0.692
0.21	3001	5.246	0.839	5.061	0.965	0.713
0.23	3001	5.252	0.84	5.03	0.958	0.731
0.25	3001	5.258	0.841	4.999	0.951	0.745
0.27	3001	5.264	0.842	4.968	0.944	0.757
0.29	3001	5.269	0.843	4.935	0.937	0.766
0.31	3001	5.274	0.844	4.901	0.929	0.773
0.33	3001	5.279	0.845	4.864	0.921	0.779
0.35	3001	5.283	0.845	4.825	0.913	0.782
0.37	3001	5.287	0.846	4.785	0.905	0.784
0.39	3001	5.291	0.847	4.742	0.896	0.784

Conclusion

The result of this study was to confirm that the mathematical models and software to solve them, which were originally developed for screw compressor design, are equally effective for use as a robust, flexible and accurate computer program to estimate the flow and thermodynamic performance of vacuum and multiphase pumps. The software has been

shown to be applicable to a variety of pump rotor profiles, including multilobe units, and is now included in an existing package, used as an aid to the design of a variety of types of positive displacement machines.

Literature

- [1] Feng C, Peng X, Xing Z. and Shu P, 2001, Thermodynamic performance simulation of a twin-screw multiphase pump, Proceedings of IMechE, Part E, Journal of Power and Energy, Vol 215, pp 157
- [2] Kovacevic A, Stosic N. and Smith I. K. and, 2006: Screw Compressors, Three Dimensional Computational Fluid Dynamics and Solid Fluid Interaction, Springer Verlag, Heidelberg
- [3] Stosic N, Smith I. K. and Kovacevic A, 2005: Screw Compressors, Mathematical Modelling and Performance Calculation, Springer Verlag, Heidelberg